Available online at www.sciencedirect.com
ScienceDirect
Solid State Communications 143 (2007) 522–526
solid state communications
www.elsevier.com/locate/ssc

Weak charge-ordering behavior in phase separated $(Ln_{1/3}Sm_{2/3})_{2/3}Ca_{1/3}MnO_3$ (Ln = Pr and La) manganites

Saket Asthana[a,b], Joonghoe Dho[a], D. Bahadur[b,c,*]

[a] Department of Physics, Kyungpook National University, Daegu, 702-701, South Korea
[b] Department of Metallurgical Engineering and Materials Science, Indian Institute of Technology, IIT Bombay, Powai, Mumbai 400076, India
[c] Institut de Chimie de la Matière Condensée de Bordeaux, UPR CNRS 9048 - Université Bordeaux 1, 87 Av. Doc. A. Schweitzer, F-33608 Pessac, France

Received 11 May 2007; received in revised form 23 June 2007; accepted 9 July 2007 by D.D. Sarma
Available online 13 July 2007

Abstract

We have studied a weak charge-ordering behavior in phase separated $(Ln_{1/3}Sm_{2/3})_{2/3}Ca_{1/3}MnO_3$ (Ln = Pr and La) manganites with same hole doping but slightly different tolerance factors. The $M(T)$ and $\rho(T)$ curves of the Pr-sample showed an anomaly caused by a weak charge-order (CO) transition at ~210 K, while that of La-sample did not. However, the La-sample displayed a weak anomaly related to the CO instability in the derivative curve of the temperature dependent magnetoresistance. This result is understood on the basis that the CO phase in La-sample is partly suppressed by a large magnetic field of ~80 kOe, while in Pr-sample it is not collapsed in that field scale. Our data support the existence of charge-ordering, electronic phase separation and a field-induced reduction of weak CO instability for La-sample, which can contribute towards high MR especially at lower temperatures due to partial melting of CO phase and/or percolation behavior.

PACS: 73.43.Qt; 75.47.Gk; 75.47.Lx; 74.25.Ha

Keywords: A. Manganites; D. Magnetoresistance; D. Colossal magnetoresistance; D. Electronic phase separation

1. Introduction

The hole doped perovskite manganites of general formula $Ln_{1-x}B_xMnO_3$ (Ln = rare earth and B = divalent alkaline earth cation) have drawn a great deal of interest because of their colossal magnetoresistance (CMR), charge-ordering (CO), electronic phase separation (EPS), etc. These systems also have technological importance for applications such as in magnetic sensors and especially for increasing the sensitivity of magnetic data read heads [1,2].

Recently, the CO and electronic phase separation phenomena in manganites have become a subject of intense research [3–5]. These intriguing phenomena are associated with strong correlation between charge, lattice, and orbital degrees of freedom. In particular, the CO behavior has been mainly observed for some commensurate fraction of carrier concentration, such as $x = 1/8, 1/2, 1/3$, etc. [6]. However, it is known that the formation of CO state is also possible for other incommensurate values of carrier concentration like in $Pr_{0.6}Ca_{0.4}MnO_3$ [7] and $Sm_{0.65}Ca_{0.35}MnO_3$ [8]. The CO state can be destabilized by a large magnetic field and hence the CO melting behavior gives rise to a large negative magnetoresistance (MR). The primary ingredients behind the formation of CO state are derived from the competition between double exchange (DE) and superexchange (SE) among the spins of manganese and the Coulomb interaction between electrons of different orbitals of the same manganese site [9,10]. The strong competition between DE and SE interactions leads to a magnetic frustration which is also responsible for the electronic phase separation [3,6]. The effects of average A-site ionic size and associated disorder in rare earth ion varied manganites have been studied to understand the nature of phase separation [11]. The phase separation in these manganites is possibly triggered by size disorder arising from the substitution of a smaller ionic size cation at the A-site.

The physical properties of doped manganites can be tailored either by A-site or by B-site substitution. The CO and EPS phenomena can be interestingly induced by A-site substitution which tunes the hole doping ratio or the average A-site ionic

* Corresponding author at: Department of Metallurgical Engineering and Materials Science, Indian Institute of Technology, IIT Bombay, Powai, Mumbai 400076, India
E-mail address: dhirenb@iitb.ac.in (D. Bahadur).

0038-1098/$ - see front matter © 2007 Elsevier Ltd. All rights reserved.
doi:10.1016/j.ssc.2007.07.008

size [12]. The average ionic size of the A-site cation and the ionic size mismatch at the A-site modify the Mn–O–Mn bond angle and affect the e_g electron hopping between Mn^{3+} and Mn^{4+} degenerate states. The effect of ionic size variation can also be understood by the tolerance factor defined as, $\tau = (\langle r_A \rangle + r_O)/\sqrt{2}(r_B + r_O)$, where r_O and r_B are radii of the oxygen and the B-site transition metal ions, respectively. It has been reported that the compounds having tolerance factor of $\leq$0.907 (in nine fold coordination number), may exhibit instabilities in the physical properties such as charge-ordering, electronic phase separation, etc. [13,14]. The A-site cation disorder is responsible for the lattice distortion which leads to the localization of e_g electrons and hence to electronic phase separation in these materials [3,6,15]. Control of hole doping ratio by A-site substitution with different valence state ions is the most straightforward experimental method for systematically tuning the properties of these materials. However, it is worthy to note that the ionic size control at a fixed hole doping ratio is another interesting experimental method to change physical properties of doped manganites.

In this paper, we have investigated the effect of varying ionic size on the magnetic and transport properties of $(Ln_{1/3}Sm_{2/3})_{2/3}Ca_{1/3}MnO_3$ (Ln = Pr and La) systems which have slightly smaller tolerance factor than the critical tolerance factor of 0.907. Here, we fixed the hole doping ratio at $x = 1/3$ but modified the value of tolerance factor, i.e., $\tau = 0.901$ for Pr-sample and $\tau = 0.903$ for La-sample, respectively. These systems exhibit interesting behaviors of charge-ordering and electronic phase separation which are sensitive to the magnetic field.

2. Experimental details

The polycrystalline samples were synthesized by the chemical citrate-gel route using high purity La_2O_3, Pr_6O_{11}, Sm_2O_3, $CaCO_3$ and Mn-acetate. The as-prepared powders were calcined at 1000 °C in air for two hours. The powders were pelletized in the form of rectangular bars and sintered at 1200 °C in air. X-ray diffraction patterns of the samples were recorded using Cu Kα radiation (PW 3040/60 Philips, PANalytical). Resistivity measurements at different applied magnetic fields were carried out between 5 and 320 K using the standard four-probe dc method (PPMS, Quantum Design). Magnetic measurements were made using vibrating sample magnetometer (Oxford, Maglab VSM) at different fields and in the temperature range of 5–300 K.

3. Results and discussion

Fig. 1 shows the X-ray diffraction patterns for $(Pr_{1/3}Sm_{2/3})_{2/3}Ca_{1/3}MnO_3$ (Pr-sample) and $(La_{1/3}Sm_{2/3})_{2/3}Ca_{1/3}MnO_3$ (La-sample) with the same hole doping ratio. All the lines in the patterns could be indexed on the basis of an orthorhombic structure (space group *Pnma*). The ionic size variance describes the effects of disorder due to disparity or mismatches of individual A-site cation radii. It is typically expressed as $\sigma^2(r_A) = x(1-x)(r_{Ln} - r_B)^2$, where r_{Ln} and r_B are the ionic radii of rare earth and divalent ions [16]. The ionic size variances of the samples are 0.15×10^{-2} Å^2 for Pr-sample and 0.08×10^{-2} Å^2 for La-sample respectively, which suggest that Ca-substituted compounds belong to the low e_g electron bandwidth manganites [5]. The cell and structural parameters of the compounds were refined by the Rietveld method using the computer code FULLPROF [17]. The lattice parameter difference between two samples is only about 0.36%. The average bond distance (Mn–O) of both samples was roughly the same but the Mn–O–Mn bond angle was slightly different. It should be noted that the variation in structural parameters is caused by the difference in the ionic size between La^{3+} and Pr^{3+}, which results in a small difference in the average A-site ionic size and thus the tolerance factor ($\tau = 0.901$ for Pr-sample and $\tau = 0.903$ for La-sample). The detailed refined parameters are given in the Table 1.

Fig. 2 shows the zero-field cooled (ZFC) and field cooled (FC) magnetization for $(Ln_{1/3}Sm_{2/3})_{2/3}Ca_{1/3}MnO_3$ (Ln = Pr and La) measured in a magnetic field of 100 Oe. The

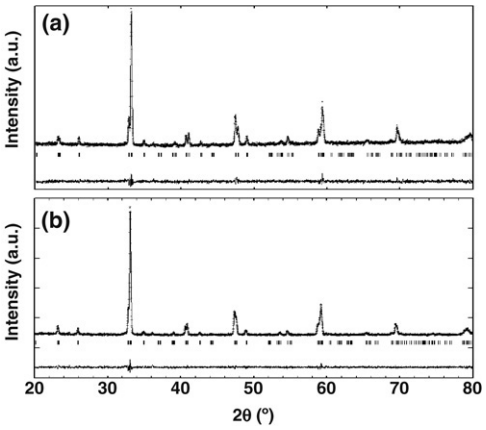

Fig. 1. Observed (symbol) and fitted (line) X-ray diffraction pattern of $(Ln_{1/3}Sm_{2/3})_{2/3}Ca_{1/3}MnO_3$ (a) Ln = Pr and (b) Ln = La using *Pnma* space group.

Table 1
Refined lattice and reliability parameters using Rietveld method for $(Ln_{1/3}Sm_{2/3})_{2/3}Ca_{1/3}MnO_3$ (Ln = Pr and La)

	$(Ln_{1/3}Sm_{2/3})_{2/3}Ca_{1/3}MnO_3$	Ln = Pr	Ln = La
	a (Å)	5.450(03)	5.450(04)
	b (Å)	7.610(09)	7.630(01)
	c (Å)	5.400(03)	5.380(05)
	V (Å^3)	223.13(28)	224.55(09)
Ln/Sm/Ca	x	0.0397	0.0364
	z	0.0042	0.0040
O1	x	−0.0190	−0.0144
	z	0.5921	0.5893
O2	x	0.2122	0.2116
	y	−0.0443	−0.0339
	z	0.7833	0.7846
	⟨Mn–O⟩	1.965(10)	1.9601(30)
	⟨Mn–O–Mn⟩	153.08(7)	155.43(3)
Reliability factors			
	R_p	3.02	3.04
	R_{exp}	3.23	3.18
	S	1.17	1.20

magnetization (M) clearly shows irreversibility between the zero-field cooled (ZFC) and the field cooled (FC) states below 150 K. This irreversibility becomes very strong below around 40 K. The appearance of irreversibility in magnetization could be attributed to magnetic frustration due to competing ferromagnetic (FM) and antiferromagnetic (AFM) interactions as found in the neutron diffraction studies on $Pr_{0.7}Ca_{0.3}MnO_3$ [18]. Remarkably, a broad hump related to another phase transition feature was observed at around 210 K for Pr-sample as seen in Fig. 2. For $Pr_{0.65}Ca_{0.35}MnO_3$, the CO transition at $T_{CO} \sim 230$ K followed by the AF transition at ∼165 K has been observed [19]. $Sm_{0.65}Ca_{0.35}MnO_3$ has also a similar CO temperature at $T_{CO} \sim 250$ K [8]. Previous studies suggest that the T_{CO} shows a slight variation with the average A-site ionic size $\langle r_A \rangle$. The values of $\langle r_A \rangle$ for Pr-sample and La-sample are 1.158 Å and 1.167 Å, respectively, which are slightly larger than that of $Sm_{0.65}Ca_{0.35}MnO_3$ ($\langle r_A \rangle = 1.148$ Å). Hence, the T_{CO} of our samples is roughly in agreement with the earlier studies. Therefore, we conjecture that the $M(T)$ curve of our Pr-sample displays a signature corresponding to AFM ordering (T_N) around 150 K. The small but weak anomaly corresponding to AFM ordering is also observed in La-sample around 150 K as shown in Fig. 2(b). On the other hand, the anomaly corresponding to the CO state in the Pr-sample is clearly observed around 210 K while it is not observable in the La-sample. Such a difference should be due to the difference in the average ionic size and thus the tolerance factor. The larger ionic size of the La ion compared to the Pr ion leads to a more symmetric crystal structure and a much weaker CO behavior for the former.

The common feature, a broad minimum around 100 K corresponding to the competing AFM and FM phases, is observed in the ZFC plots for both samples [20]. The width of the minima is larger in Pr-sample, which suggests stronger frustration of FM phase in Pr-sample than in La-sample. Another prominent feature is a large increase in magnetization below 50 K particularly in the FC data for both the samples, which is associated with the onset of FM ordering as observed by Cao et al. [21] for $Pr_{5/8}Ca_{3/8}MnO_3$ manganites. This result suggests the coexistence of charge-ordered antiferromagnetic phase (CO-AFM) with FM phase at low temperature.

Insets of Figs. 2(a) and (b) show the plots of inverse of ZFC dc susceptibility versus temperature measured with a field of 100 Oe for $(Ln_{1/3}Sm_{2/3})_{2/3}Ca_{1/3}MnO_3$ (Ln = Pr and La) samples. It is worth noting that the inverse susceptibility deviates from the Curie–Weiss (C–W) law especially at $T < T_{CO}(T_N)$ with paramagnetic temperature (θ_p) ∼ 96 K and ∼ 73 K for Pr-sample and La-sample, respectively. This indicates the presence of magnetic inhomogeneities in our samples, which is typically taken to be an evidence of phase separation [22]. We conjecture that some FM clusters are possibly created in the field cooled process but in the ZFC process the host AF phase begins to develop at T_N and suppresses some FM clusters below the irreversibility temperature.

The temperature dependences of electrical resistivity, $\rho(T)$, for the Pr- and La-sample in 0 kOe and 80 kOe fields are shown in Fig. 3. For the former, the zero-field $\rho(T)$ curve

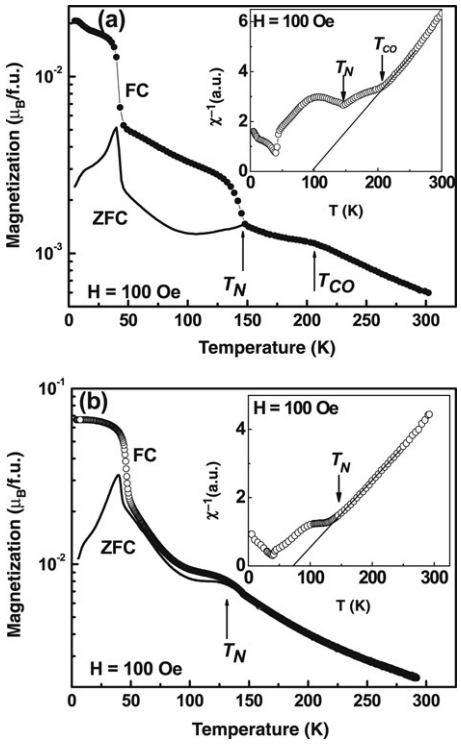

Fig. 2. Variation of magnetization in ZFC and FC cycles with temperature in 100 Oe for $(Ln_{1/3}Sm_{2/3})_{2/3}Ca_{1/3}MnO_3$ (a) Ln = Pr and (b) Ln = La. Insets show the inverse susceptibility variation with temperature. T_N and T_{CO} are the temperatures corresponding to the AFM and CO phase transitions, respectively.

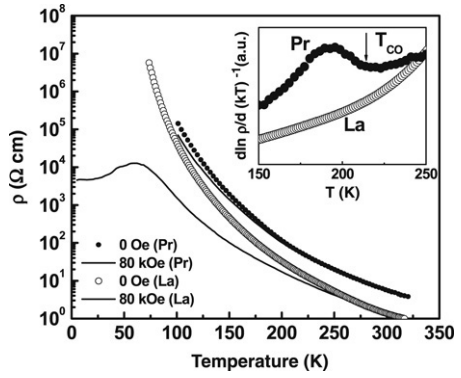

Fig. 3. Variation of resistivity with temperature in zero-field and 80 kOe field for $(Ln_{1/3}Sm_{2/3})_{2/3}Ca_{1/3}MnO_3$ (Ln = Pr and La). The inset displays the $d\ln\rho/d(k_BT)^{-1}$ plot which shows an anomaly corresponding to CO transition which is clear in Pr-sample.

displays a weak upturn signature below ∼210 K, which can be observed in the $d\ln\rho/d(k_BT)^{-1}$ plot (inset of Fig. 3). The position of the anomaly temperature is roughly in agreement with the charge-ordering temperature of the parent compound $Pr_{0.67}Ca_{0.33}MnO_3$ [23,24]. On the other hand, La-sample did not show any signature for CO transition in both plots, indicating that the CO behavior in La-sample is much weaker than that in Pr-sample. It has been reported that the compounds having tolerance factors around or less than 0.907 (in nine fold coordination number) may exhibit charge-order phenomena [6]. On this basis, both the samples should belong to the CO compound category as the tolerance factor is 0.901 for

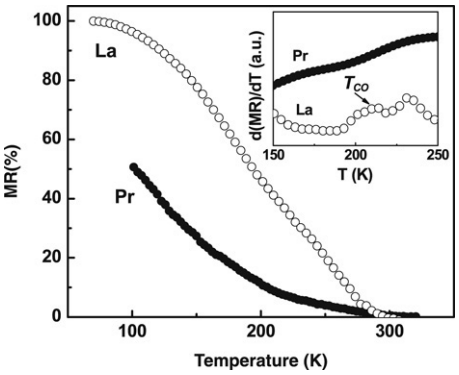

Fig. 4. Variation of percentage of MR with temperature in 80 kOe field for $(Ln_{1/3}Sm_{2/3})_{2/3}Ca_{1/3}MnO_3$ (Ln = Pr and La). The inset shows the derivative plot of temperature dependent magnetoresistance.

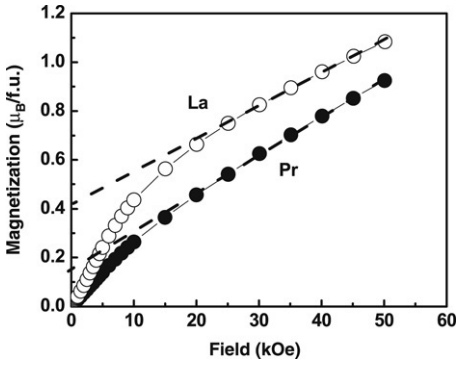

Fig. 5. Virgin magnetization plots for $(Ln_{1/3}Sm_{2/3})_{2/3}Ca_{1/3}MnO_3$ (Ln = Pr and La) at 5 K. The dashed line shows a linear fitting for the magnetization data above 20 kOe.

Pr-sample and 0.903 for La-sample, respectively. But, the La-sample does not show any anomaly for the CO transition in $\rho(T)$ and $\mathrm{d}\ln\rho/\mathrm{d}(k_BT)^{-1}$ plots. This suggests that the anomaly of CO transition in resistivity and magnetization data gradually weakens as the tolerance factor approaches the critical tolerance factor of 0.907.

The resistivity of the Pr-sample showed a very small decrement even in a large magnetic field of 80 kOe (Fig. 3) while that of the La-sample displayed a large drop, i.e., a field-induced insulator–metal transition which is caused by the melting behavior of CO state as typically observed in $Pr_{1-x}Ca_xMnO_3$ for $x = 0.3$–0.5 [25,26]. It seems that for Pr-sample the critical field for a CO melting behavior is much larger than 80 kOe. Fig. 4 displays temperature dependent magnetoresistance (MR) for Pr- and La-samples measured at a field of 80 kOe. The MR values for both the samples gradually increase with the decrease of temperature. The inset of Fig. 4 displays the derivative of the temperature dependent MR data, $\mathrm{dMR}(T)/\mathrm{d}T$. The $\mathrm{dMR}(T)/\mathrm{d}T$ of the Pr-sample did not show any significant feature corresponding to the CO transition while that of La-sample showed an anomaly at around 200 K although the derivative data was very noisy. The point of anomaly position in the $\mathrm{dMR}(T)/\mathrm{d}T$ plot of the La-sample is very similar to the CO temperature of the Pr-sample. Therefore, we conjecture that the anomaly observed in the $\mathrm{dMR}(T)/\mathrm{d}T$ plot for the La-sample is probably due to a weak CO instability. A large magnetic field of 80 kOe can remove the weak CO instability of La-sample and thus the $\mathrm{dM(R)}/\mathrm{d}T$ plot can display an anomaly at T_{CO}. Pr-sample, on the other hand, with stronger CO characteristics cannot show any anomaly in $\mathrm{dMR}(T)/\mathrm{d}T$ curve because a field of 80 kOe is not large enough to induce a collapse of the CO phase. It is remarkable that the La-sample displays a weak anomaly in $\mathrm{dMR}(T)/\mathrm{d}T$ plot although it does not display an observable signature related to the CO transition in $M(T)$, $\rho(T)$ and $\mathrm{d}\ln\rho/\mathrm{d}(k_BT)^{-1}$ plots.

Fig. 5 displays the virgin magnetization curve for Pr- and La-samples as a function of magnetic field at 5 K measured up to a field of 50 kOe. A non-linear increase was observed at low field region (<10 kOe), while non-saturating and nearly linear behaviors were found at high field region (>10 kOe). Both samples should have very small but finite FM moment at zero-field because a linear fitting for the magnetization data above 10 kOe (dashed line) does not pass the zero point. This may be due to the presence of well-separated charge delocalized ferromagnetic clusters in the antiferromagnetic insulating matrix [27]. Both the non-linearity and FM moment are slightly larger for the La-sample than the Pr-sample. The FM clusters align to the field direction at low field and gradually grow within the AFM matrix with increasing magnetic field. The reduction in the saturation magnetization from its expected theoretical value ($3.7\mu_B$) is a signature of electronic and magnetic inhomogeneities induced by the A-site cation size variance. This behavior had been observed in $(Ln_{1-x}Ln_x)_{0.7}Ca_{0.3}MnO_3$ (Ln = Nd, Gd and Y) compounds and is thought to be a typical evidence of electronic phase separation with a rather short-range FM order [9,28].

The CO-AFM state is generally collapsed by an application of a large magnetic field. In the present study, we observed the melting behavior of the CO-AFM state only for the La-sample within the range of applied magnetic field. In Fig. 6, we displayed the $M(H)$ loops for the La-sample at three temperatures to understand the CO melting behavior. The temperatures of 80, 60 and 5 K have been chosen on the basis of features observed in M–T and ρ–T data. At 80 K, the $M(H)$ data shows a linear dependence even at relatively low field region (<10 kOe). As the temperature decreases to 60 and 5 K, the low field magnetization curves gradually change from a linear function to a non-linear function, implying a gradual development of FM clusters. Such a non-linearity in the low field $M(H)$ data implies the coexistent states of FM and AFM phases at low temperature. A similar behavior is observed by Fan et al. [29] in the B-site doped manganites, $Nd_{0.5}Ca_{0.5}Mn_{1-x}Cr_xO_3$ which is a typical charge-ordered compound. On the other hand, the high field $M(H)$ loop shows a metamagnetic transition behavior from AFM to FM state above ~80 kOe and a large hysteresis upon the field sweep, indicating a sudden expansion of the FM phase at the expense of the AFM (CO) phase. The points of inflexions in both the cycles are found to be at ~80 kOe, which corresponds to a critical field to observe the CO melting behavior as seen in the resistivity data. The maximum moment is still much smaller than the theoretically expected saturation moment, indicating that the competition between FM and AFM phases is still present in

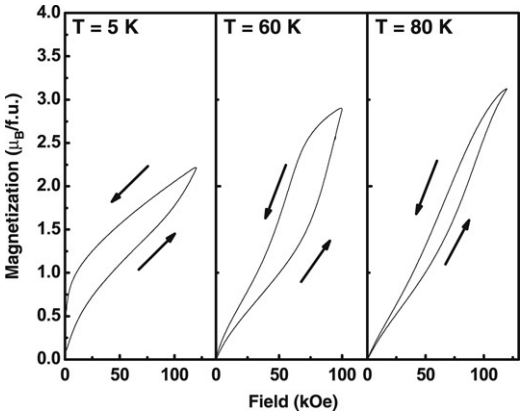

Fig. 6. Magnetic hysteresis loops for $(La_{1/3}Sm_{2/3})_{2/3}Ca_{1/3}MnO_3$ at 5, 60 and 80 K. The critical field required for CO melting is about ∼80 kOe, which is estimated from a change in slope.

the experimental magnetic field range. Hence, a weak CO-AFM feature gets support from the magnetization plot. The CO-state in La-sample seems to be weak and metastable which can be melted by sufficiently high magnetic fields.

The possible microscopic origin of the critical phenomena like CO and EPS in these low e_g bandwidth manganites can be described by the double well (FM and CO-AFM) potentials model [30]. The energy difference between the AFM and FM potential well (Δ) can be a responsible factor to decide the stability of the phase at a given temperature (k_BT) and field ($-\mu H$). According to our observations, we can infer that Δ is larger in Pr-sample as compared to La-sample. Therefore, the CO-AFM phase in the La-sample can be melted by a field of about 80 kOe, while the CO phase in Pr-sample is more robust due to larger Δ and does not show the melting behavior of CO phase in our field limits.

4. Conclusions

We have synthesized the phase separated manganites $(Ln_{1/3}Sm_{2/3})_{2/3}Ca_{1/3}MnO_3$ (Ln = Pr and La) samples which crystallize in the orthorhombic structure (space group *Pnma*). For Pr-sample, a weak anomaly due to charge-ordering was observed around 210 K in $M(T)$ and $\rho(T)$ data. On the other hand, the La-sample did not show any anomaly related to the CO transition in $M(T)$ and $\rho(T)$ data but interestingly showed a weak anomaly in the derivative plot of magnetoresistance, which may be caused by a field-induced reduction of the weak CO instability. The existence of electronic phase separation in our samples is supported by the non-saturating magnetization as well as the non-linearity of $M(H)$ plot. The irreversibility in ZFC and FC magnetization behavior and the strong dependence of resistivity on magnetic field at low temperatures are suggestive of electronic phase separation. The two competing interactions, namely, the CO-AFM coupling that favors insulating phase and the FM coupling that favors metallic phase, presumably lead to electronic phase separation.

Acknowledgements

SA and DB are grateful to the Department of Science and Technology, India for support of this project. This work was partly supported by the BK21 research programme and by a grant (RO1-2006-000-10369-01) from the Basic Research Programme of the KOSEF.

References

[1] J. Heremans, J. Phys. D 26 (1993) 1149.
[2] S. Jin, M. McCormack, T.H. Tiefel, R. Ramesh, J. Appl. Phys. 76 (1994) 6929.
[3] E. Dagotto (Ed.), Nanoscale Phase Separation and Colossal Magnetoresistance, Springer, Berlin, 2003.
[4] A.P. Ramirez, J. Phys.: Condens. Matter 9 (1997) 8171.
[5] V.B. Shenoy, D.D. Sharma, C.N.R. Rao, Chem. Phys. Chem. 7 (2006) 2053.
[6] C.N.R. Rao, B. Raveau (Eds.), Colossal Magnetoresistive, Charge Ordering and Related Properties of Manganese Oxides, World Scientific, Singapore, 1998.
[7] J. Dho, N.H. Hur, Solid State Commun. 140 (2006) 469.
[8] C. Martin, A. Maignan, M. Hervieu, B. Raveau, Phys. Rev. B 60 (1999) 12191.
[9] J. vandenBrink, D. Khomskii, Phys. Rev. Lett. 82 (1999) 1016.
[10] J. vandenBrink, G. Khaliullin, D. Khomskii, Phys. Rev. Lett. 83 (1999) 5118.
[11] L. Sudheendra, C.N.R. Rao, J. Phys.: Condens. Matter 15 (2003) 3029.
[12] S. Asthana, D. Bahadur, A.K. Nigam, S.K. Malik, J. Appl. Phys. 97 (2005) 10H711.
[13] J.M. De Teresa, M.R. Ibarra, J. Garcia, J. Blasco, C. Ritter, P.A. Algarabel, C. Marquina, A. Del Moral, Phys. Rev. Lett. 76 (1996) 3392.
[14] J.M. Dai, W.H. Song, J.J. Du, J.N. Wang, Y.P. Sun, Phys. Rev. B 67 (2003) 144405.
[15] S. Asthana, A.K. Nigam, S.K. Malik, D. Bahadur, J. Alloys Compounds (2007) (in press).
[16] J.P. Attfield, Cryst. Eng. 5 (2002) 427.
[17] Juan Rodríguez-Carvajal, Laboratoire Léon Brillouin (CEA-CNRS) CEA/Saclay, 91191 Gif sur Yvette Cedex, France, version 2006.
[18] D.E. Cox, P.G. Radaelli, M. Marezio, S.-W. Cheong, Phys. Rev. B 57 (1998) 3305.
[19] R. Kajimoto, T. Kakeshita, Y. Oohara, H. Yoshizawa, Y. Tomioka, Y. Tokura, Phys. Rev. B 58 (1998) R11837.
[20] V. Dediu, C. Ferdeghini, F.C. Matacotta, P. Nozar, G. Ruani, Phys. Rev. Lett. 84 (2000) 4489.
[21] G. Cao, J. Zhang, S. Cao, C. Jing, X. Shen, Appl. Phys. Lett 86 (2005) 042507.
[22] J. Burgy, M. Mayr, V. Martin-Mayor, A. Moreo, E. Dagotto, Phys. Rev. Lett. 87 (2001) 277202.
[23] C. Jardon, F. Rivadulla, L.E Hueso, A. Fondado, M.A. Lopez-Quintela, J. Rivas, R. Zysler, M.T Causa, R.D. Sanchez, J. Magn. Magn. Mater. 196–197 (1999) 475.
[24] F. Rivadulla, M.A. Lopez-Quintela, L.E Hueso, C. Jardon, A. Fondado, J. Rivas, M.T. Causa, R.D. Sanchez, Solid State Ion. 110 (1999) 179.
[25] Y. Tomioka, A. Asamitsu, H. Kuwahara, Y. Moritomo, Phys. Rev. B 53 (1996) R1689.
[26] A.M.L. Lopes, J.P. Araujo, A.M. Gomes, M.S. Reis, V.S. Amarala, P.B. Tavares, J. Magn. Magn. Mater. 272–276 (2004) 1767.
[27] G. Li, Z. Xianyu, C. Kim, H. Kim, Y. Lee, J. Magn. Magn. Mater. 239 (2002) 51.
[28] T. Sudyoadsuk, R. Suryanarayanan, P. Winotai, L.E. Wenger, J. Magn. Magn. Mater. 278 (2004) 96.
[29] J. Fan, J. Xie, Y. Ying, L. Pi, Y. Zhang, Solid State Commun. 138 (2006) 299.
[30] J. Dho, N.H. Hur, Phys. Rev. B 67 (2003) 214414.